© 2017. Published by The Company of Biologists Ltd | Journal of Cell Science (2017) 130, 4051-4062 doi:10.1242/jcs.208983

RESEARCH ARTICLE

FYCO1 regulates accumulation of post-mitotic midbodies by mediating LC3-dependent midbody degradation

Lai Kuan Dionne[1,*], Eric Peterman[2,*], John Schiel[3], Paulius Gibieža[4], Vytenis Arvydas Skeberdis[4], Antonio Jimeno[5], Xiao-Jing Wang[1,‡] and Rytis Prekeris[2,‡]

ABSTRACT

The post-mitotic midbody (MB) is a remnant of cytokinesis that can be asymmetrically inherited by one of the daughter cells following cytokinesis. Until recently, the MB was thought to be degraded immediately following cytokinesis. However, recent evidence suggests that the MB is a protein-rich organelle that accumulates in stem cell and cancer cell populations, indicating that it may have post-mitotic functions. Here, we investigate the role of FYCO1, an LC3-binding protein (herein, LC3 refers to MAP1LC3B), and its function in regulating the degradation of post-mitotic MBs. We show that FYCO1 is responsible for formation of LC3-containing membrane around the post-mitotic MB and that FYCO1 knockdown increases MB accumulation. Although MBs accumulate in the stem-cell-like population of squamous cell carcinomas, FYCO1 depletion does not affect the clonogenicity of these cells. Instead, MB accumulation leads to an increase in anchorage-independent growth and invadopodia formation in HeLa cells and squamous carcinoma cells. Collectively, our data suggest that FYCO1 regulates MB degradation, and we present the first evidence that cancer invasiveness is a feature that can be modulated by the accumulation of MBs in cancer stem cells.

This article has an associated First Person interview with the first author of the paper.

KEY WORDS: Autophagy, Cytokinesis, Midbody, Post-mitotic accumulation, Post-mitotic degradation

INTRODUCTION

Abscission is the process of separating the two daughter cells during the final stages of cell division. This is a highly controlled event that requires coordinated endosomal transport and cytoskeleton rearrangement at the abscission site and the midbody (MB) (Fededa and Gerlich, 2012; Mierzwa and Gerlich, 2014; Bhutta et al., 2014). The MB is a microtubule-rich structure that has primarily been studied for its role in regulating cytokinesis (Fededa and Gerlich, 2012; Mierzwa and Gerlich, 2014). Several cell cycle-regulating kinases, such as Aurora B and Plk1, were shown to accumulate at the MB (Fededa and Gerlich, 2012; Mierzwa and Gerlich, 2014; D'Avino and Capalbo, 2016; Hu et al., 2012). Additionally, the centralspindlin and the ESCRT complexes are also present at the MB, where they govern the ingression of the cleavage furrow as well as abscission of the intracellular bridge connecting the two daughter cells (Bhutta et al., 2014; Douglas and Mishima, 2010). It was generally believed that MBs do not have any post-mitotic roles and that immediately following division, MBs are either degraded or released into extracellular space. Surprisingly, recent work has demonstrated that post-mitotic MBs can reside in the cytoplasm long after the completion of cell division (Kuo et al., 2011; Chen et al., 2013; Ettinger et al., 2011). While the post-mitotic functions of MBs are only starting to emerge, several studies have shown that MBs may act as polarity cues during polarization of epithelial and neuronal cells (Blasky et al., 2015; Li et al., 2014; Pollarolo et al., 2011). The MB has also been implicated in promoting stemness and increasing tumorigenicity of cancer cells (Kuo et al., 2011; Ettinger et al., 2011). Consistent with this idea, stem cells and metastatic cancer cells were all shown to accumulate MBs, although it is not known whether MBs can directly regulate cell stemness (Salzmann et al., 2014). It is well established that multiple cancer stem cell populations can co-exist in tumors and that they contribute to the heterogeneity of tumor bulk (Akrap et al., 2016). These cancer stem cell populations may exert distinct proliferative or migratory phenotypes to promote tumor initiation or invasion. While studies have shown that cancer stem cells can undergo an epithelial–mesenchymal transition to switch back and forth between proliferative and migratory phenotype, tumor initiation and metastasis are two processes that can be uncoupled (Biddle et al., 2011; White et al., 2013). Therefore, the capacity of cancer stem cells to initiate tumor formation does not necessarily predict its invasive potential. Thus, MB accumulation in cancer stem cells may differentially affect these tumorigenic features.

While it is becoming clear that MBs may be important regulators of several post-mitotic cellular functions, it is not known how post-mitotic MBs are accumulated and retained in cells. Post-mitotic MBs can be obtained during asymmetric abscission when the MB is inherited by one of the daughter cells (Fig. 1A) (Dionne et al., 2015). Once inherited, the MB can be encapsulated by autophagic membranes and undergo degradation (Fig. 1A) (Kuo et al., 2011; Dionne et al., 2015). Alternatively, the MB can evade autophagy and be retained in the post-mitotic cell (Kuo et al., 2011). It is now well established that macroautophagy plays a major part in preventing accumulation of MBs. It has been reported that inhibiting autophagy by knocking down NBR1, Atg6 (also known as BECN1), Atg7 or administration of ammonium chloride or chloroquine leads to post-mitotic MB accumulation (Kuo et al., 2011; Ettinger et al., 2011). Consequently, MB accumulation has been correlated to changes in several cellular functions, including differentiation, reprogramming efficiency and colony-forming

[1]Department of Pathology, University of Colorado Anschutz Medical Campus, Aurora, CO 80045, USA. [2]Department of Cell and Developmental Biology, University of Colorado Anschutz Medical Campus, Aurora, CO 80045, USA. [3]GE Healthcare Dharmacon Inc., 2650 Crescent Drive, Suite 100, Lafayette, CO 80026, USA. [4]Institute of Cardiology, Lithuanian University of Health Sciences, Kaunas 50161, Lithuania. [5]Medical Oncology, Department of Medicine, University of Colorado Anschutz Medical Campus, Aurora, CO 80045, USA.
*These authors contributed equally to this work

‡Authors for correspondence (rytis.prekeris@ucdenver.edu; xj.wang@ucdenver.edu)

R.P., 0000-0003-3393-1963

Received 28 July 2017; Accepted 16 October 2017

Journal of Cell Science (2017) 130, 4051-4062 doi:10.1242/jcs.208983

ability. However, since autophagy is known to govern many cellular functions, it remains to be established whether these changes are a direct consequence of post-mitotic MB accumulation, or merely a side effect of generic inhibition of autophagy.

Since autophagy-dependent MB degradation directly affects post-mitotic MB retention, it is plausible that MB targeting to the autophagic degradative pathway is a highly regulated event. Furthermore, post-mitotic MBs are large structures (1–3 µm) (Schiel et al., 2011). Unlike starvation-induced autophagy, encapsulation of large cytosolic structures requires substantial targeted endocytic membrane delivery during the extension of autophagic isolation membrane and likely involves specific regulatory proteins to facilitate this process. In this study, we present evidence that FYCO1 is responsible for mediating MB degradation. FYCO1 is a FYVE domain-containing protein that binds Rab7 proteins and has been implicated in autophagy (Pankiv et al., 2010). Importantly, FYCO1 has been shown to mediate autophagic degradation of large cytosolic structures, and FYCO1 mutations lead to inclusion body myositis and autosomal-recessive congenital cataracts (Chen et al., 2011; Güttsches et al., 2016). Here, we demonstrate that FYCO1 colocalizes to post-mitotic MBs, indicating its potential role in post-mitotic MB degradation. We further found that FYCO1 mediates the formation of LC3-containing (herein, LC3 refers to MAP1LC3B) membrane around the MB and that loss of FYCO1 results in MB accumulation in HeLa cells. Importantly, loss of FYCO1 does not affect the general autophagy pathway, suggesting that FYCO1 specifically mediates degradation of large cytosolic structures and organelles, such as MBs. Identification of FYCO1 as a regulator of MB degradation allowed us to further assess the functional consequences of MB accumulation in cancer cells without inhibiting the general autophagy pathway. We used squamous cell carcinoma (SCC) as a model, since SCC cell populations are known to contain cancer stem cells. We found that the cancer stem cells of SCC cell lines accumulated more MBs than non-cancer stem cells. Loss of FYCO1 in these SCC cell lines did not lead to the expansion of side population (the stem-cell-like population) or increase the clonogenicity of SCC. Remarkably, we found that FYCO1 knockdown increased invadopodia formation in SCC spheroids. Taken together, we propose that FYCO1 mediates MB degradation. While MB accumulation in cancer stem cell does not enhance cancer cell survival or proliferation, we demonstrate that MB accumulation contributes to the regulation of cancer cell invasiveness.

RESULTS

FYCO1 is recruited during early stages of LC3-containing membrane formation around post-mitotic MBs

Recent studies have demonstrated that post-mitotic MBs can be asymmetrically inherited and retained in cells (Fig. 1A) (Kuo et al., 2011; Ettinger et al., 2011; Dionne et al., 2015). Additionally, post-mitotic MBs can be internalized from extracellular milieu and degraded by LC3-associated phagocytosis (LAP) (Crowell et al., 2014; Fazeli et al., 2016). Since these post-mitotic MBs are implicated in the regulation of various cellular functions (Kuo et al., 2011; Ettinger et al., 2011; Li et al., 2014; Pollarolo et al., 2011) MB degradation becomes an important aspect that controls MB retention and signaling (Fig. 1A) (Kuo et al., 2011; Fazeli et al., 2016; Pohl and Jentsch, 2009). However, how these large post-mitotic MB structures are specifically recognized by degradative machinery remains unclear. Thus, we decided to investigate whether MB degradation requires specialized proteins, such as FYCO1, that mediate MB recognition and targeting to the degradative pathway. FYCO1 is a FYVE-domain-containing protein that interacts with Rab7 proteins and LC3 (Fig. 1B) and has been implicated in mediating kinesin-dependent autophagosome movement and maturation (Pankiv et al., 2010; Ma et al., 2017; Olsvik et al., 2015; Da Ros et al., 2017). To determine whether FYCO1 can mediate MB degradation, we stained HeLa cells with anti-FYCO1 and anti-MKLP1 (MB marker) antibodies. We found that while many post-mitotic MBs do not associate with FYCO1-containing organelles (Fig. 1C), about 32% of post-mitotic intracellular MBs were surrounded with FYCO1-containing organelles and membrane (Fig. 1D), suggesting that FYCO1 may be involved in marking a subset of MBs for degradation. To further test this possibility, we co-transfected HeLa cells with FYCO1–mCherry and MKLP1–GFP constructs and analyzed the extent of association between post-mitotic MBs (labeled by MKLP1–GFP) and FYCO1–mCherry. As shown in Fig. 1E, some of the MBs (28% of total) were surrounded by FYCO1–mCherry-containing membranes.

FYCO1 has been implicated in regulating autophagy, and we next tested whether FYCO1 marks autophagic isolation membranes. Since LC3 is an autophagosome regulator that is recruited during initial autophagocytic cup formation, we transfected HeLa cells with LC3–mCherry and tested its colocalization with FYCO1-containing organelles. As shown in Fig. 1F, the vast majority of FYCO1–GFP-containing organelles (92% of total organelles analyzed) were also positive for LC3–mCherry. These data are consistent with previously published work demonstrating that FYCO1 binds directly to LC3 via its LIR motif and might be involved in regulating autophagy, although the exact function of FYCO1 remains to be defined (Pankiv et al., 2010). Additionally, LC3 was also shown to mediate LC3-associated phagocytosis and degradation of extracellular MBs (Fazeli et al., 2016). Thus, FYCO1 may actually mediate both autophagic and LAP-dependent post-mitotic MB degradation.

After LC3-dependent formation of isolation membrane, autophagosomes fuse with lysosomes to ensure the degradation of encapsulated cargo. Thus, we next tested whether FYCO1-containing organelles also contain lysosomal markers, such as Lamp1 and CD63. To that end, we transfected HeLa cells with FYCO1–GFP and stained them with either anti-Lamp1 or anti-CD63 antibodies. Interestingly, a substantial fraction of FYCO1-positive organelles did not contain Lamp1 or CD63 (Fig. S1). Additionally, in some cases, we could observe lysosomes docked in close proximity to FYCO1-containing organelles, presumably just before a lysosome fusion event (Fig. S1D, arrows). Since autophagosome fusion with lysosomes occurs during autophagosome maturation, it is likely that these Lamp1- and CD63-negative and FYCO1-positive organelles represent autophagosomes at the early stages of their formation or maturation. To test when FYCO1 is recruited to the autophagosomes, we next performed time-lapse imaging. FYCO1–GFP was transiently transfected into HeLa cells and FYCO1–GFP dynamics were assessed. Consistent with our previous data, FYCO1–GFP could be detected in autophagocytic ‘cups’ that were at the early stages of limiting membrane extension (Fig. 2A; the asterisk marks an opening in the forming autophagosome). After 20–40 min, these autophagocytic cups closed, leading to formation of a complete autophagic isolation membrane (Fig. 2A; see last image in time-lapse series). Significantly, analyses using short time-lapses (5 s) revealed that membranes delivered to autophagocytic cups already contained FYCO1–GFP (Fig. 2B), suggesting that FYCO1 is delivered at the early stages of isolation membrane extension and may be required for the formation of autophagosome.

We next assessed whether lysosomes fuse with autophagosomes after the recruitment of FYCO1–GFP. To that end, we co-transfected HeLa cells with FYCO1–GFP and Lamp1–mCherry,

Journal of Cell Science

Journal of Cell Science (2017) 130, 4051-4062 doi:10.1242/jcs.208983

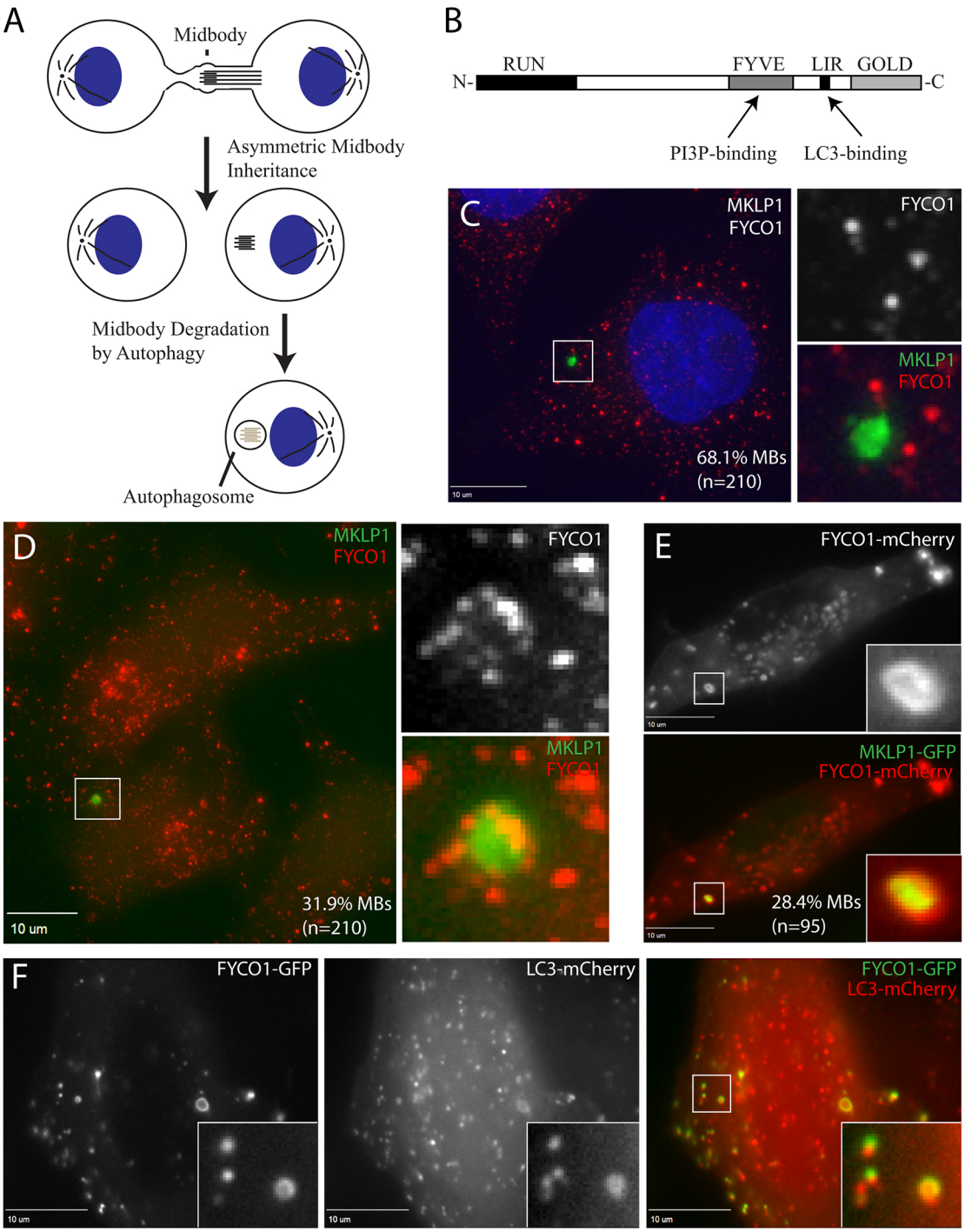

Fig. 1. FYCO1 is present on MB-containing autophagosomes. (A) Schematic representation of asymmetric post-mitotic MB inheritance and subsequent degradation via autophagy. (B) Schematic representation of the FYCO1 domain structure. (C,D) HeLa cells were fixed and stained with anti-MKLP1 (MB marker) and anti-FYCO1 antibodies. The box marks the subcellular regions shown in insets. The number at the bottom right of the images show the percentage of all MBs that either do not colocalize (C) or colocalize (D) with FYCO1-containing membranes. (E) HeLa cells transiently co-expressing FYCO1–mCherry and MKLP1–GFP were fixed, and colocalization between FYCO1 and MKLP1 was analyzed. (F) HeLa cells transiently co-expressing FYCO1–GFP and LC3–mCherry were fixed, and colocalization between FYCO1 and LC3 was analyzed.

and analyzed the dynamics of lysosomes and autophagosomes in live cells. Consistent with our previously mentioned data, some large FYCO1–GFP-labeled autophagosomes were devoid of Lamp1–mCherry (Fig. 2C, asterisk) and likely represent early stages of autophagosome maturation. Interestingly, lysosomes would only dock and fuse with FYCO1-containing autophagosomes that already contained lysosomal markers and were likely in late stages of autophagosome maturation (Fig. 2D,E; arrows mark lysosomes). Collectively, these data demonstrate that FYCO1 is recruited to the forming autophagocytic cup and that FYCO1 may be involved in the extension of the isolation membrane during autophagosome assembly around post-mitotic MBs.

Journal of Cell Science (2017) 130, 4051-4062 doi:10.1242/jcs.208983

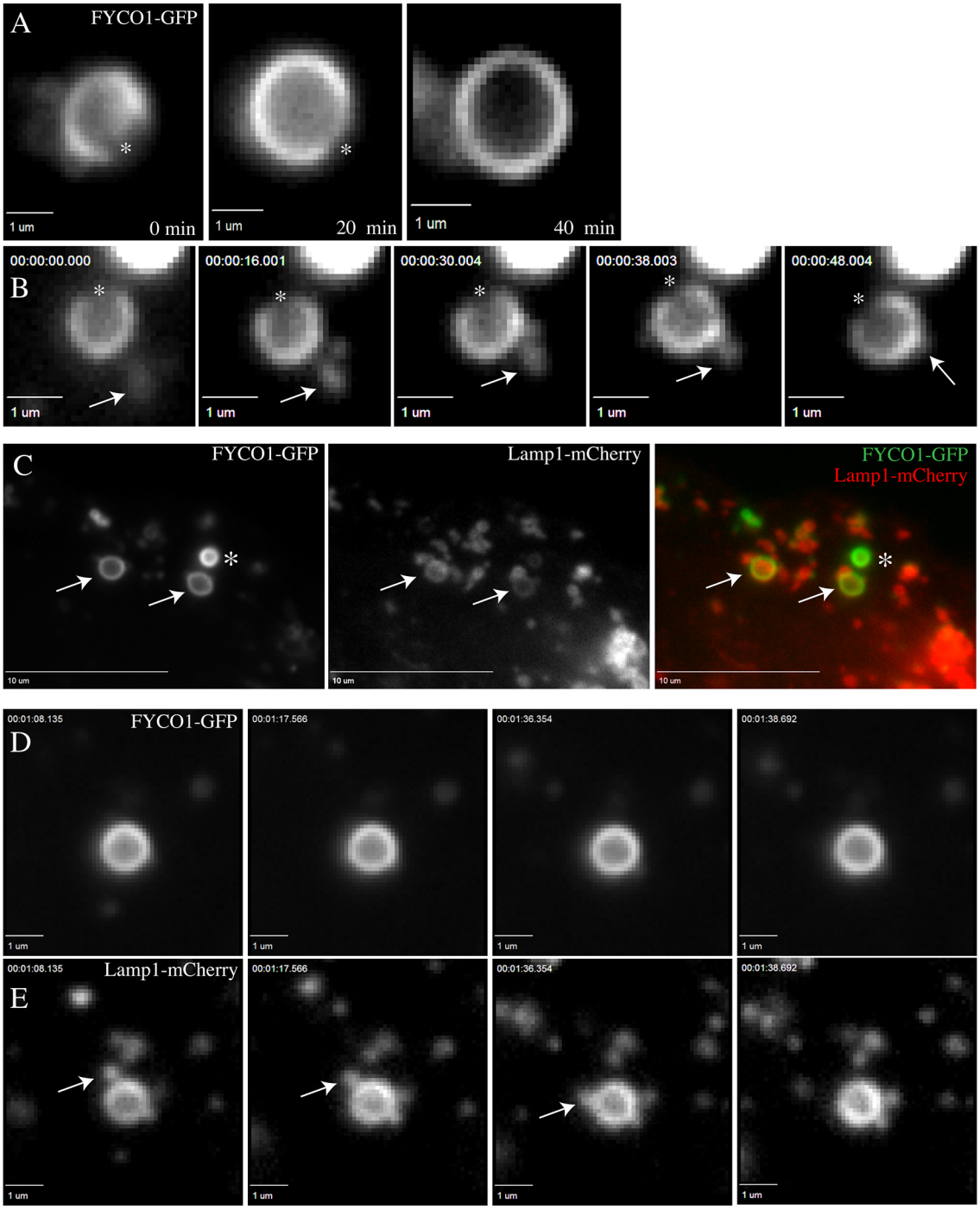

Fig. 2. FYCO1 is recruited to the isolation membrane during early stages of autophagocytic cup formation. (A,B) Time-lapse imaging reveals that FYCO1–GFP is already present at the isolation membrane by the time of extension of the autophagocytic cup. Shorter interval time-lapse imaging (B) reveals that FYCO1–GFP is present at the small endocytic organelles that are delivered and fuse with autophagocytic cups during their extension and closure. Asterisks in A and B mark the opening in the autophagocytic cup. Arrows in B indicate endocytic membranes that fuse with autophagocytic cups. (C) HeLa cells transiently co-expressing FYCO1–GFP and Lamp1–mCherry were fixed and colocalization between FYCO1 and Lamp1 was analyzed. Asterisks indicate early autophagosome that contains FYCO1–GFP but not Lamp1–mCherry. (D,E) Lamp1 recruitment to autophagosomes occurs only after autophagosome closure. Cells were transiently co-transfected with FYCO1–GFP (D) and Lamp1–mCherry (E). Images from time-lapse series showing the recruitment and fusion of Lamp1–mCherry-containing lysosomes with FYCO1–GFP-containing autophagosomes. Arrows point to the lysosome and autophagosome fusion event.

FYCO1 is required for LC3-dependent degradation of post-mitotic MBs

Since our data demonstrate that FYCO1 colocalizes with post-mitotic MBs, we next tested the role of FYCO1 in mediating MB degradation. To that end, we created HeLa cell lines stably expressing two different FYCO1 shRNAs (FYCO1-KD1 and FYCO1-KD2) (Fig. S2C). We began by assessing the number of MBs in mock versus FYCO1-depleted cells. To do so, we used HeLa cells stably expressing MKLP1–GFP, a well-established MB marker. As shown in Fig. 3A,B, FYCO1 knockdown led to a

Journal of Cell Science

Journal of Cell Science (2017) 130, 4051-4062 doi:10.1242/jcs.208983

statistically significant increase in the number of MBs per cell. Since FYCO1 may be involved in mediating autophagosome or LAP maturation, we also analyzed the percentage of post-mitotic MBs that were encapsulated by CD63-positive membrane (a marker for lysosomes and mature autophagosomes/phagosomes). As shown in Fig. 3D,E, FYCO1 depletion led to a decrease in the percentage of post-mitotic MBs contained within CD63- or LC3-positive organelles. While these data suggest that FYCO1 is mediating MB degradation, the alternative possibility is that FYCO1 may affect cytokinesis, thus indirectly affecting the number of post-mitotic MBs. However, we observed that FYCO1 does not associate with the MB during cytokinesis (Fig. S2A,B). Similarly, FYCO1

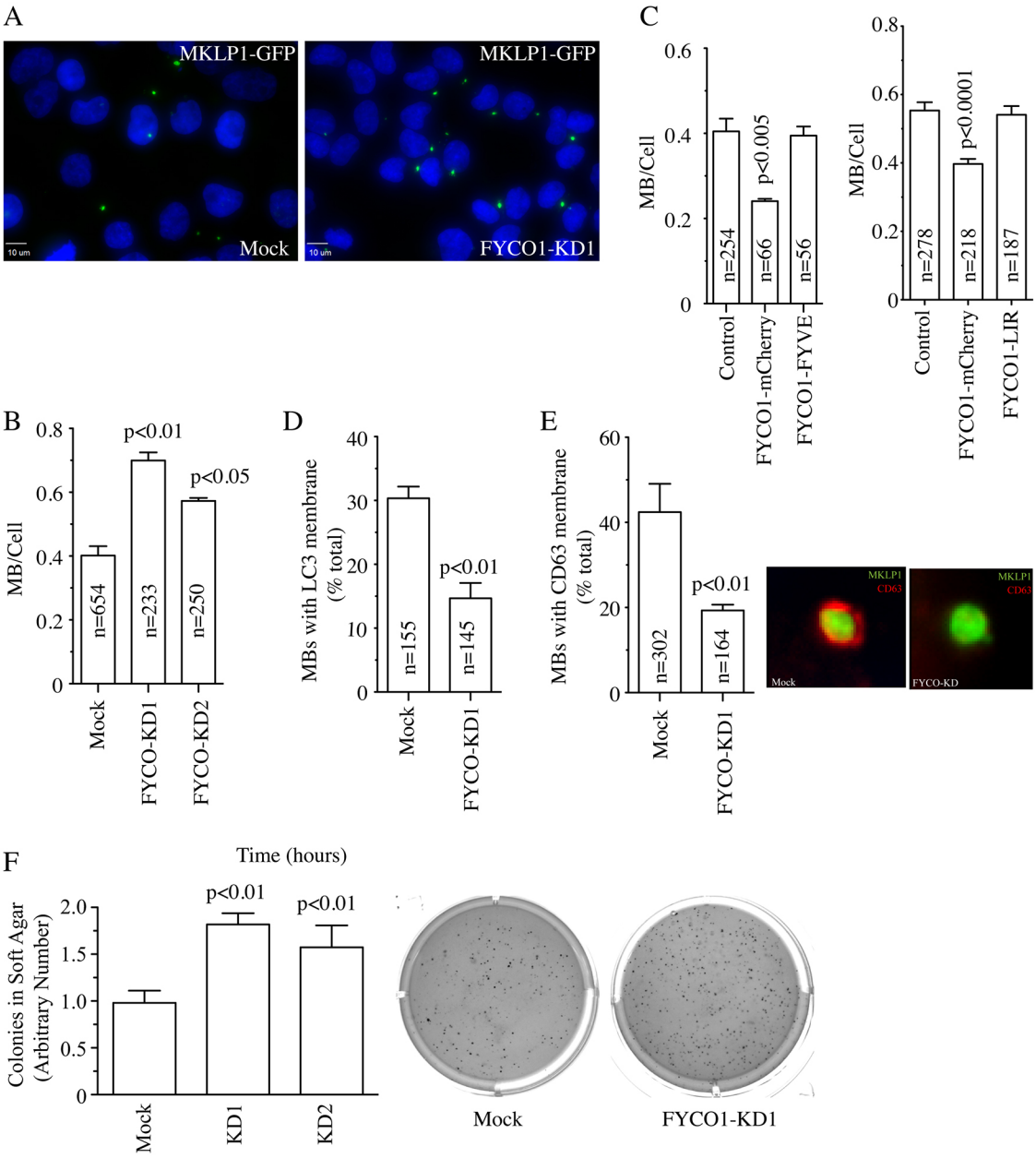

Fig. 3. FYCO1 mediates post-mitotic MB degradation by autophagy. (A,B) HeLa cells stably expressing FYCO1 shRNAs (FYCO1-KD1 and FYCO1-KD2) and MKLP1–GFP were analyzed for the absence or presence of post-mitotic MBs. Data is expressed as the ratio between MBs and nuclei in each randomly chosen field. Data shown in B are the mean±s.d. derived from three independent experiments. *n* is the total number of cells counted. (C) HeLa cells expressing MKLP1–GFP cells were mock or transiently transfected with FYCO1–mCherry or the FYCO1-FYVE mutant or FYCO1-LIR mutant. Cells were then analyzed for the presence or absence of the MBs. Data are expressed as the ratio between nuclei and MBs in each randomly chosen field. Data shown are the mean±s.d. derived from three independent experiments. *n* is the total number of cells counted. (D,E) HeLa cells stably expressing FYCO1 shRNAs and MKLP1–GFP cells were stained with anti-CD63 antibody, a lysosomal marker (E), or with anti-LC3 antibody, an autophagy/LAP marker (D). The number of MBs present within CD63- or LC3-positive phagolysosomes were then counted. Data shown are the mean±s.d. derived from three independent experiments. *n* is the total number of post-mitotic MBs counted. The images in E show the colocalization of CD63 and MKLP1–GFP-positive midbody in mock transfected HeLa-MKLP1–GFP cells. This colocalization is decreased when cells are transfected with FYCO1 shRNAs. (F) FYCO1 knockdown results in an increase in anchorage-independent growth. HeLa cells stably expressing FYCO1 shRNAs were plated into soft agar and allowed to grow for 2 weeks. Colonies were then stained with Nitrotetrazolium Blue chloride and quantified via ImageJ. The number of colonies per plate were then counted and compared to control HeLa cells. Data shown are the mean±s.d. derived from three independent experiments. Representative image of plates are shown on the right. *P*-values shown in this figure were calculated with a Student's *t*-test.

Journal of Cell Science (2017) 130, 4051-4062 doi:10.1242/jcs.208983

knockdown does not lead to a change in the percentage of multi-nucleated cells or cells in telophase when compared to mock-transfected cells (Fig. S2D). All these data rule out the possibility that FYCO1 regulates cytokinesis or the cell cycle, and suggest that the effects of FYCO1 depletion on post-mitotic MB number are due to inhibition of autophagosome/LAP-mediated MB degradation.

So far, we have demonstrated that FYCO1 is required for MB degradation. We next asked whether inducing high expression of FYCO1 can stimulate targeting of MBs to the degradative pathway and deplete the MBs. Indeed, overexpression of FYCO1–mCherry in HeLa cells expressing MKLP1–GFP (MKLP1 is also known as KIF23) led to a significant decrease in the number of MBs per cell in comparison to control cells (Fig. 3C). Additionally, this FYCO1–mCherry-induced decrease in post-mitotic MBs was dependent on FYCO1 binding to LC3 and phosphatidylinositol 3-phosphate (PI3P) since FYCO1-LIR and FYCO1-FYVE domain deletion mutants did not have any effect on intracellular MB accumulation (Fig. 3C). These data collectively demonstrate that FYCO1 is necessary for MB degradation. Importantly, FYCO1 knockdown did not have any effect on basal autophagic flux (Fig. 2E), suggesting that FYCO1 exerts a specific function by regulating the extension of the autophagic isolation membranes around large cytosolic structures, such as MBs.

Depletion of FYCO1 leads to an increase in cancer cell invasiveness but not clonogenicity

Several studies have demonstrated that accumulation of post-mitotic MBs can lead to changes in various cell functions (Kuo et al., 2011; Ettinger et al., 2011). An intriguing suggestion is that MB retention and accumulation may be required for retaining or even inducing stem-cell-like properties in cancer cells (Kuo et al., 2011). However, interpretation of some of these findings has been difficult since many studies used either general autophagy inhibitors (such as chloroquine and/or NH_4Cl) or siRNAs to deplete core autophagic components [such as p62 (also known as SQSTM1) and/or ATG6] to test the role of MB accumulation (Kuo et al., 2011; Ettinger et al., 2011; Pohl and Jentsch, 2009). Since depletion of FYCO1 increased the number of post-mitotic MBs without affecting general autophagic flux, we next sought to use FYCO1-depleted cells to further examine the functional consequences of MB accumulation. Consistent with previous reports that MB accumulation increases tumorigenic potential, depletion of FYCO1 in HeLa cells led to increase in colony formation in soft agar, a method commonly used to assess anchorage-independent growth and survival of cancer cells (Fig. 3F).

We proceeded to test the effect of FYCO1 depletion and MB accumulation on regulating the formation and/or maintenance of cancer stem cells. To that end, we chose squamous cell carcinomas (SCCs) as an experimental model since the presence of cancer stem cells is one of the characteristics of SCCs (White et al., 2013). To determine whether cancer stem cells from SCCs accumulate post-mitotic MBs, we used cell lines (B931 and B911) derived from genetically engineered mice carrying two frequent SCC mutations, that is, a Kras-activating mutation and Smad4 deletion, in the keratin-15-expressing bulge stem cell (White et al., 2013). Previous xenograft experiments showed that B931 is highly metastatic to the lungs, whereas B911 is less metastatic in nature (White et al., 2013). We detected the Hoechst 33342 dye-excluding side population from B911 by performing a fluorescence-activated cell sorting (FACS) analysis (Fig. 4A). These cells are considered cancer stem cells due to their expression of ABC transporters and hence they have the ability to efflux drugs or dyes. Verapamil, an inhibitor of ABC transporters that prevents efflux of Hoechst 33342 dye, was used as a control to confirm the side population (Fig. 4A,B). We then sorted both the non-side population and side population, and cultured these cells as spheroids. As shown in Fig. 4C, the side population was able to form larger and more rounded spheroids when compared to the non-side population. Using MKLP1 as a MB marker, we performed whole-mount immunofluorescence on these spheroids and analyzed the number of MBs per spheroid area (Fig. 4C). We found that the side population spheroids retained significantly more MBs than the non-side population (Fig. 4C). Similarly, we were able to identify that the side population from B931 also accumulated more MBs than the non-side population (Fig. 4D,E). To investigate whether MB accumulation is also seen in human cancer stem cells, we isolated cancer stem cells from the patient-derived head and neck SCC line CUHN013 based on enhanced aldehyde dehydrogenase (ALDH) activity (Fig. S3A). Similar to our observation in B911 and B931 cell lines, the ALDH-high cancer stem cells possessed a better spheroid-forming ability than ALDH-low cells (Fig. S3B). Importantly, the ALDH-high cancer stem cells also accumulated more MBs when compared to ALDH-low cell population (Fig. S3B). Taken together, these findings are consistent with the hypothesis that MBs are more prone to retain in the cancer stem cell populations (Kuo et al., 2011; Ettinger et al., 2011).

Since the side populations of SCCs accumulate MBs, we next wondered whether MB accumulation could be sufficient to enrich these cancer stem cell pools. To test that, we created B911 and B931 cell lines stably expressing FYCO1 shRNA (Fig. 5A). Similar to what was observed for HeLa cells, FYCO1 knockdown resulted in increased MB accumulation (Fig. 5B; Fig. S4A) while having no effect of general autophagic flux (Fig. 5C). Importantly, FYCO1 depletion had an especially strong effect on accumulation of post-mitotic MBs (Fig. 5B), suggesting that FYCO1 regulates MB degradation in SCCs. Next, we tested the effect of FYCO1 depletion in inducing the size of side populations in SCCs. Depletion of FYCO1 did not expand the side populations in SCC lines (as measured by flow cytometry; data not shown). To further test the effect of FYCO1, we also used a clonogenic assay that is routinely used to assess the ability of colony formation in cancer stem cells (Franken et al., 2006). Consistent with the side population analysis, FYCO1 depletion did not have any effect on the clonogenic properties of B911 cells and actually decreased the clonal growth of B931 cells (Fig. S4B). Thus, our study suggests that post-mitotic MB accumulation alone does not appear to increase the side populations in SCCs.

Since FYCO1 depletion and the subsequent MB accumulation affected the anchorage-independent growth of HeLa cells, we next asked whether loss of FYCO1 could also affect the invasiveness of SCCs. To test this possibility, we embedded B931 cells into 3D Matrigel–collagen matrix and assessed their ability to form invadopodia, which are finger-like protrusions necessary for cancer cells to ultimately metastasize (Jacob et al., 2013, 2016). Since B911 are poorly metastatic and did not form spheroids in Matrigel–collagen matrix (data not shown), we excluded this cell line from further analysis and focused only on the highly metastatic B931 cells. Remarkably, depletion of FYCO1 in the B931 cells significantly increased their ability to form invadopodia and this effect was reversed upon the introduction of shRNA-resistant FYCO1–GFP (Fig. 5D,E). Taken together, these data suggest that the accumulation of MBs in cancer stem cells upon the depletion of FYCO1 increases the invasive potential of cancer. Based on our findings, cancer stem cells may actively modulate the autophagy pathway to promote MB accumulation and increase cancer

Journal of Cell Science

Journal of Cell Science (2017) 130, 4051-4062 doi:10.1242/jcs.208983

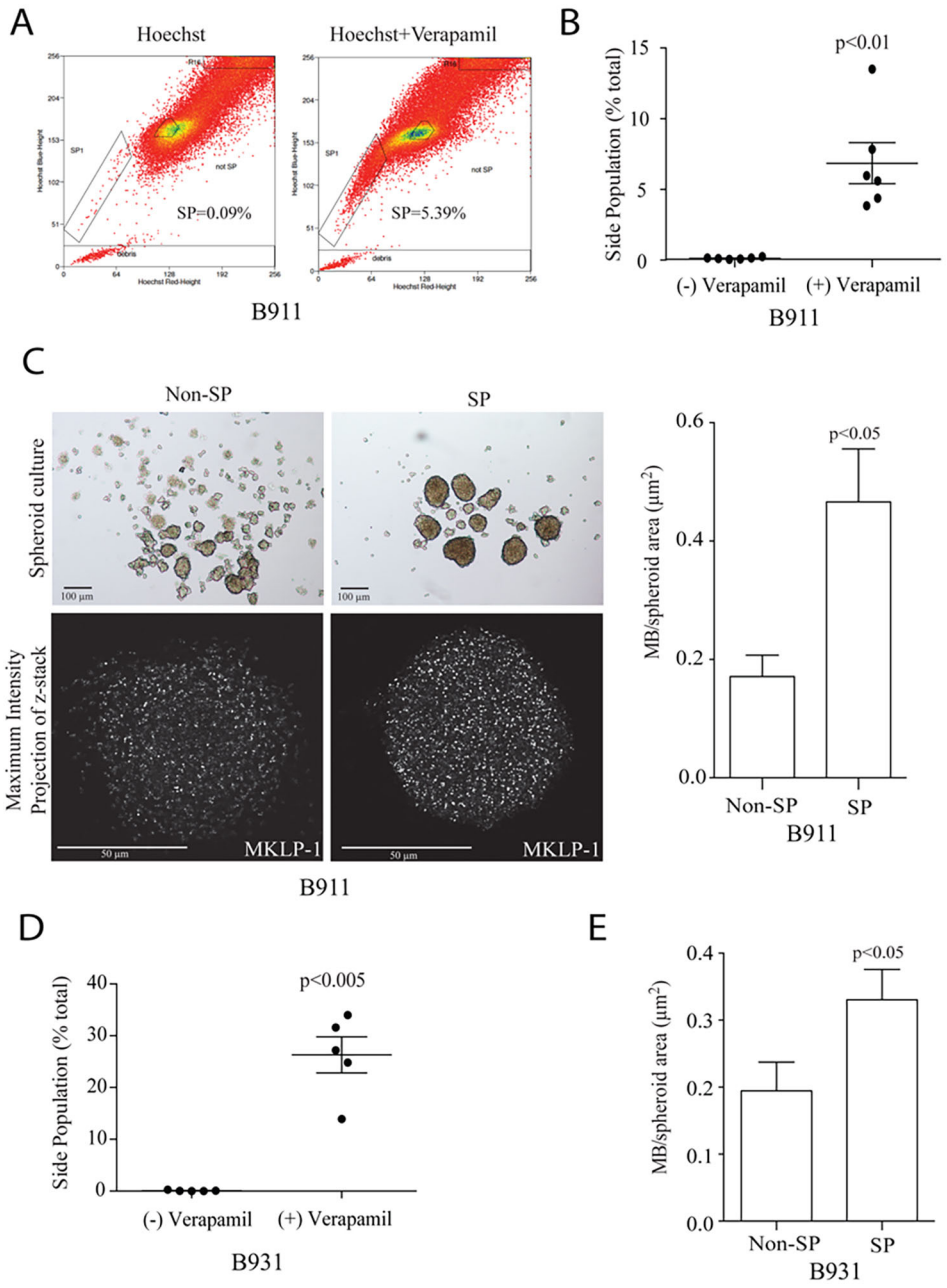

Fig. 4. The stem-cell-like side population of B911 and B931 SCC cells accumulate post-mitotic MBs. (A,B) Live B911 cells were stained with Hoechst 33342 in the presence or absence of Verapamil. Cells were then analyzed by flow cytometry and cells negative for Hoechst 33342 dye were gated as SPs. (B) Quantification of flow cytometry analysis. Data shown are the mean±s.d. from six independent experiments. (C) Flow-sorted non-side population (SP) and SP B911 cells were cultured on ultra-low attachment six-well plates to allow formation of spheroids (top panels). Note that SPs form larger spheroids than do non-SPs. SP and non-SP spheroids were then fixed, and stained using anti-MKLP1 antibodies to visualize post-mitotic MBs. Images shown are maximum intensity projections along the *z*-axis. The bar graph shows a quantification of MB number in B911 SP- and non-SP-derived spheroids. Data shown are the mean±s.d. number of MBs per spheroid are from three independent experiments. (D) Quantification of the percentage of flow-sorted B931 SP and non-SP cells (as described in A). (E) Quantification of MB number in spheroids derived from B931 SP and non-SP cells. Data shown are the mean±s.d. from three independent experiments. *P*-values shown in this figure were calculated with a Student's *t*-test.

invasiveness. This hypothesis is further exemplified by the downregulation of FYCO1 in many cancers, including head and neck, and esophagus squamous cell carcinomas (Fig. S4C,D).

DISCUSSION

Until recently, the MB was thought to play an important role only during mitotic cell division and that it was discarded into the extracellular milieu or immediately degraded following completion of cytokinesis. However, recent studies suggested that post-mitotic MBs actually have important roles during cell differentiation and organogenesis (Kuo et al., 2011; Li et al., 2014; Mangan et al., 2016). One of the best-described roles for the post-mitotic MB is to act as a polarity cue during neurite outgrowth and epithelia morphogenesis (Pollarolo et al., 2011; Mangan et al., 2016). Indeed, it is now well-established that post-mitotic MBs mark the apical lumen formation site during the development of epithelial and hepatic ducts (Mangan et al., 2016). Another intriguing, but largely unexplored, role of MBs is its function as a stemness or tumorigenic factor. It has been proposed that inhibition of macroautophagy-dependent MB degradation leads to cells acquiring stem-like properties (Kuo et al., 2011; Ettinger et al., 2011). However, the stemness-inducing properties of post-mitotic MBs are still very controversial, largely due to the fact that in all studies accumulation of MBs was induced by inhibiting the entire autophagy pathway (Kuo et al., 2011; Ettinger et al., 2011; Pohl and Jentsch, 2009). As a consequence, it is difficult to tease apart the specific effects of MB accumulation on the cells from the general effects of autophagy inhibition. Additionally, stemness of cancer cells is often broadly defined, and cancer stem cells have been shown to exhibit distinct proliferative or migratory phenotypes depending on molecular cues. Thus, it becomes extremely challenging to directly elucidate the roles of post-mitotic MBs in preserving stemness. In this study, we focused on identifying and characterizing the factors that target post-mitotic MBs for degradation. Here, we identify FYCO1 as an

Journal of Cell Science (2017) 130, 4051-4062 doi:10.1242/jcs.208983

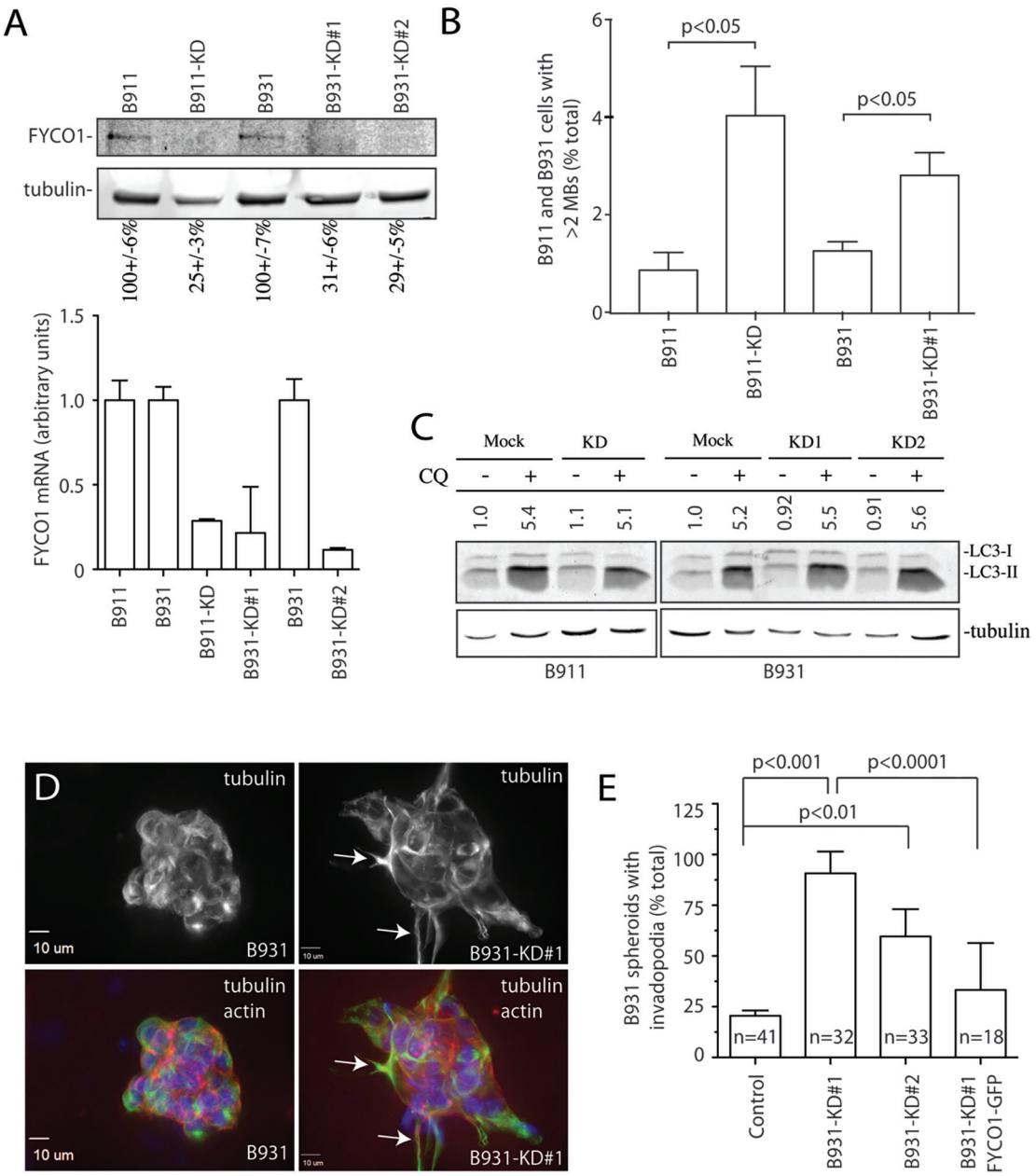

Fig. 5. FYCO1 knockdown increases invasiveness of B931 cells. (A) qPCR and western blots confirming the extent of FYCO1 knockdown in the SCC lines B911 and B931. Data shown are the mean±s.d. percentage levels compared to control lines (set at 100%, for western blots, or 1, for qPCR) derived from three different western blots of qPCR analyses. (B) B911 and B931 cells stably expressing FYCO1 shRNAs cells were analyzed for the absence or presence of two or more post-mitotic MBs as determined by staining with anti-MKLP1 antibody. Data shown are the mean±s.d. derived from three independent experiments. (C) To test the effect of FYCO1 knockdown on autophagic flux, cells were grown in the presence or absence of 40 µM chloroquine (CQ) for 8 h. Cells were then lysed, and levels of LC3-II (activated LC3) were analyzed by western blotting. Numbers listed above blots are levels of LC3-II (arbitrary units) normalized against tubulin (loading control) and the untreated wild-type control. (D,E) To test the effect of FYCO1 knockdown on the invasiveness of B931 cells, B931 control, FYCO1 shRNA-expressing or FYCO1 shRNA co-expressed with shRNA-resistant FYCO1–GFP cells were resuspended in Matrigel–collagen mixture and allowed to grow for 5 days. Formed spheroids were then fixed and stained with Hoechst 33342, phalloidin conjugated to Alexa Fluor 568 and anti-β-tubulin antibody to assess invadopodia formation. D shows representative images of control or FYCO1 shRNA-expressing cells. Arrows point to invadopodia. E shows quantification of the number of spheroids that formed at least one invadopodia. Data shown are the means and standard deviations from three independent experiments. *n* is the number of spheroids analyzed. *P*-values shown in this figure were calculated with a Student's *t*-test.

important regulator of MB degradation that does not playing a role in general autophagic flux, which allow us to specifically test how loss of FYCO1 affect different properties of cancer cell stemness and tumorigenicity.

FYCO1 is a FYVE-domain-containing protein that is known to bind to Rab7 and LC3 and is thought to mediate microtubule-dependent autophagosome transport and maturation (Pankiv et al., 2010; Ma et al., 2017). However, the functions of FYCO1 are not well examined and remain largely unclear. Mutations in FYCO1 have been associated with genetic diseases such as congenital cataracts and inclusion-body myositis (Chen et al., 2011; Güttsches et al., 2016). These disorders are defined by the accumulation and/or

Journal of Cell Science (2017) 130, 4051-4062 doi:10.1242/jcs.208983

aggregation of organelles and cytosolic proteins leading to various complications such as inflammation, autoimmunity and formation of cataracts in lens cells. Based on these symptoms, it was proposed that FYCO1 may function in mediating autophagic degradation of large cytosolic structures. Since MBs are 1–3 µm in diameter, we hypothesized that FYCO1 is a potential protein that mediates MB degradation while having no effect on basal autophagic flux. Consistent with this hypothesis, we determined that FYCO1 colocalizes with LC3 and the post-mitotic MB in HeLa cells. Significantly, we also show that FYCO1-containing organelles are delivered to the forming autophagosomes at early stages of autophagy by fusing with isolation membrane during the extension of autophagocytic cups.

After demonstrating that FYCO1 colocalizes and appears to mediate the enveloping of post-mitotic MBs in autophagosomes, we next tested the idea that loss of FYCO1 would increase the number of post-mitotic MBs. Consistent with the involvement of FYCO1 in MB degradation, FYCO1 knockdown led to an increase of post-mitotic MBs, while having no effect on general autophagic flux. Additionally, overexpression of FYCO1–GFP led to a decrease in the accumulation of post-mitotic MBs. Finally, FYCO1 depletion decreased the number of MBs present within the phagolysosome. Based on all these data, we propose that FYCO1 is involved in mediating the delivery and fusion of endocytic organelles during the formation or extension of autophagocytic cups, thus providing the membranes needed to form the isolation membrane around MBs during their degradation (Fig. 6). It is important to note that recently LC3 was implicated in regulating a specialized phagocytic pathway (LC3-associated phagocytosis or LAP) that mediates the internalization and degradation of extracellular MBs (Fazeli et al., 2016). Thus, it is tempting to speculate that FYCO1 may actually be mediating both MB degradation pathways, specifically autophagic degradation of inherited MBs and LAP-associated degradation of internalized MBs (Fig. 6). Further studies will be needed to test this possibility.

As previously mentioned, it is now well established that post-mitotic MBs can function as a polarity cue in several polarized cells (Li et al., 2014; Pollarolo et al., 2011). However, its role as a stemness or tumorigenic factor remains much more controversial. Some work indicates that stem cells accumulate MBs, while other work suggests that certain stem cell populations actually release them more frequently (Kuo et al., 2011; Ettinger et al., 2011). Additional work observing germline stem cell populations in *Drosophila melanogaster* embryos suggests that regulation of MB accumulation depends on the sex of the organism (Salzmann et al., 2014). The identification of FYCO1 as a factor that regulates MB degradation without affecting general autophagy gives us a unique opportunity to test how post-mitotic MBs affect the induction or maintenance of cell stemness. To that end, we decided to use squamous cell carcinoma (SCC) as a model since the presence of cancer stem cells is one of the characteristics of SCCs. We first isolated the side-population (stem-cell-like population) from two different mice SCC cell lines and assessed the post-mitotic MB number. We found that MB number was significantly increased in the side population as compared to the rest of the SCC cells. Importantly, MBs were also increased in stem-cell-like population (isolated based on ALDH levels) of the human SCC cell line CUHN013, suggesting that the ability to accumulate MBs is likely a general property of cancer stem cells in all SCCs.

While SCC cancer stem cells do accumulate post-mitotic MBs, it remains unclear whether this accumulation actually promotes cancer cell stemness. More specifically, we wondered how post-mitotic MBs might differentially affect the various spectra of cancer cell stemness, such as the proliferation and migration phenotypes. To examine that, we depleted FYCO1 in both mice SCC cell lines and tested the size of side population as well as their ability to grow in clonogenic assays. We found that FYCO1 depletion had no effect on the size and expansion of side population and the clonogenicity of these SCCs were not affected as well. Therefore, our data suggest that post-mitotic MBs are not required for the induction or maintenance of SCC stem cell populations. If post-mitotic MBs do not affect SCC clonogenicity, then what function, if any, do they play? It was previously suggested that accumulation of MBs may induce anchorage-independent cell growth (Kuo et al., 2011). Consistent with this hypothesis, our data shows that FYCO1 depletion induced MB accumulation in HeLa cells and promoted

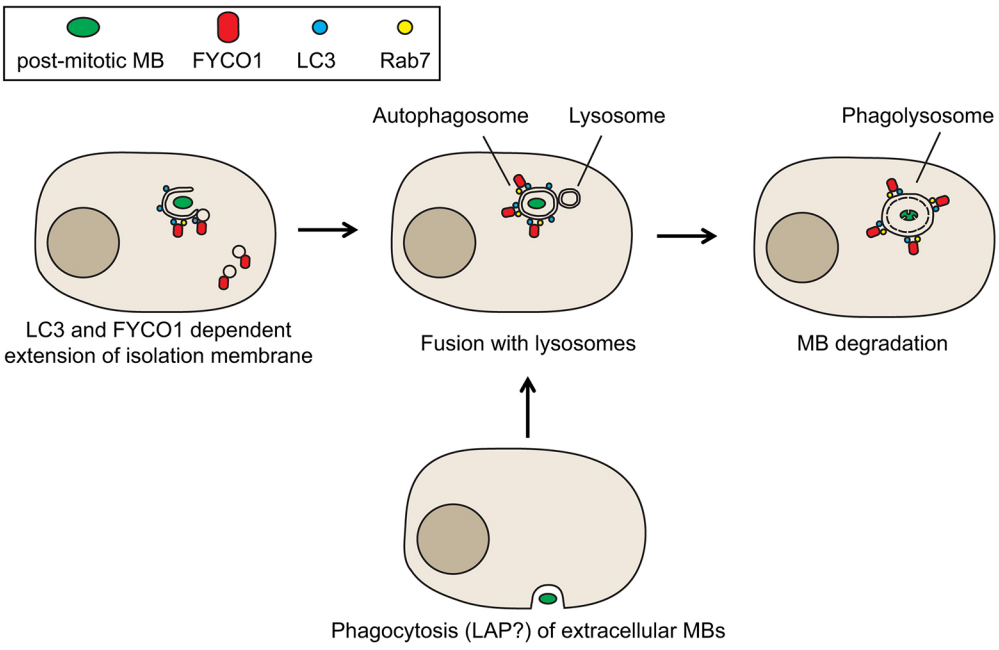

Fig. 6. Proposed model of FYCO1-dependent post-mitotic MB degradation. FYCO1-containing endosomes are targeted to forming autophagocytic cup to allow extension of the isolation membrane around post-mitotic MBs marked for autophagosomal degradation. This process is likely mediated by binding of FYCO1 to lipidated LC3 present in autophagocytic cup. MB-containing autophagosomes then mature by fusing with lysosomes, eventually leading to MB degradation. Note that we cannot rule out the possibility that at least some of the post-mitotic MBs are internalized from the extracellular milieu and degraded via the LC3-associated phagocytic (LAP) pathway. Since FYCO1 binds directly to LC3 it is likely that LAP-dependent MB degradation may also require FYCO1.

Journal of Cell Science (2017) 130, 4051-4062 doi:10.1242/jcs.208983

colony growth in soft-agar, suggesting that post-mitotic MB accumulation may increase cancer cell invasiveness. As another measure of tumorigenic or invasive potential, we embedded SCCs into a Matrigel–collagen mixture and assessed the effect of FYCO1 knockdown on their invasiveness. In line with the idea that MBs may enhance cancer cell tumorigenicity, loss of FYCO1 increased invadopodia formation in B931 spheroids. The side population of B931 was previously identified as the metastatic cancer stem cells of SCC that had a migratory phenotype. Therefore, accumulation of MBs in the side population of B931 cells may promote cancer invasiveness and lead to enhance metastasis.

Taken together, our data clearly demonstrate that MBs can regulate post-mitotic cellular functions and that autophagy or LAP-dependent MB degradation is likely a highly regulated process that relies on FYCO1. Furthermore, we showed that MB accumulation affects the different aspects of stemness in cancer. Given that fly germline stem cells differentially accumulate MBs based on the sex of the fly (Salzmann et al., 2014), this supports the idea that the MB is not necessarily involved solely in the maintenance of stemness. Rather, post-mitotic MB accumulation may impart different functions depending on the cell types that are also affected by environmental and developmental factors. Further work will be needed to better understand the regulation and function of the post-mitotic MBs, especially as it pertains to stemness and tumorigenicity.

MATERIALS AND METHODS

Cell culture

HeLa, B911 and B931 cells were grown as described previously (White et al., 2013; Schiel et al., 2012) and were routinely tested for mycoplasma contamination. CUHN013 cells were grown at 37°C in 5% CO_2 with Dulbecco's modified Eagle's medium with F12 (DMEM/F12) supplemented with 10% fetal bovine serum (FBS), 10 ng/ml human epidermal growth factor (hEGF), 5 µg/ml transferrin, 5 µg/ml insulin and 0.4 µg/ml hydrocortisone. HeLa MKLP1–GFP cells were a generous gift from Stephen Doxsey (University of Massachusetts Medical School, USA) (Kuo et al., 2011). Stable FYCO1 knockdown B911 and B931 cell lines (B911-KD and B931-KD) were generated by using Sigma lentiviral mouse FYCO1 shRNA plasmids (TRCN0000047529 and TRCN0000178746). Stable FYCO1 knockdown HeLa cell lines (HeLa-KD1 and HeLa-KD2) were generated by using Sigma lentiviral mouse human FYCO1 shRNA plasmids (TRCN0000038916 and TRCN0000038915). For rescue experiments, FYCO1–GFP was transiently transfected into HeLa-KD or B931-KD1 cells by using Lipofectamine 2000 (ThermoFisher Scientific, Waltham, MA). Cells were then sorted into a GFP+ population with a MoFlo XDP100 machine and used in subsequent 3D invadopodia formation assays. For spheroid culture, 5×10^3 sorted cells were resuspended in 2 ml of spheroid medium (DMEM/F12 with 10 ng/ml bFGF and 20 ng/ml EGF) and added to an ultra low attachment six-well plate (Corning). Spheroids were replenished with fresh medium every 4 days and analyzed at day 10 post plating.

Soft agar growth assays

Soft agar assays were performed as described previously (Borowicz et al., 2014). Briefly, cells were resuspended in Phenol Red-free medium and mixed with Noble agar solution (BD Biosciences, cat# 214220) to reach a final density of 8×10^3 cells per ml of 0.2% agar–medium solution. Cells were then overlaid on previously solidified 0.2% agar–medium layer in six-well plates. Once the agar–cell layer had solidified, the cells were then overlaid with 2 ml of Phenol Red-free complete medium. Cells were then allowed to grow for 2 weeks, and colonies were then visualized by staining with Nitrotetrazolium Blue chloride. The number of colonies was counted by using ImageJ software. Colony number was counted and averaged from three different technical replicates in each experiment. The data shown are the means derived from three different experiments.

Cancer stem cells analysis

To identify the side population, B911 and B931 cells were cultured to subconfluency and trypsinized. Cells were reconstituted with FACS buffer (PBS with 3% FBS) at a concentration of 10^6 cells/ml. Cells were stained with 25 ng/ml of Hoechst 33342 dye (Sigma-Aldrich) and the mixture was incubated at 37°C for 1.5 h with mixing every 15 min. Control cells were stained as above but with the addition of 50 µM Verapamil (Sigma-Aldrich) to inhibit Hoechst 33342 dye efflux. After incubation, cells were washed and reconstituted with FACS buffer and filtered through a 40 µm cell strainer. Prior to FACS analysis, propidium iodide (Sigma-Aldrich) was added at a final concentration of 10 µg/ml to select for live cells. Cells were analyzed by using a MoFlo XDP70 flow cytometer (Beckman Coulter). The side population and non-side population were distinguished and sorted based on the Hoechst 33342 dye efflux profile with or without addition of Verapamil. Data was evaluated by using Summit software (v 6.2).

To identify cancer stem cells with high ALDH activity, we utilized the ALDEFLUOR™ kit (Stemcell Technologies) according to the manufacturer's protocol. CUHN013 cells were cultured to subconfluency and harvested with trypsin. Cells were reconstituted with ALDEFLUOR™ assay buffer at a concentration of 10^6 cells/ml and 5 µl of activated ALDEFLUOR™ reagent was added. Then, 0.5 ml of cell mixture were taken and added to 5 µl of ALDEFLUOR™ diethylaminobenzaldehye (DEAB) reagent to establish the ALDH-high cell population. The cell mixture was incubated at 37°C for 1 h and prepared for FACS analysis as described above.

Immunohistochemistry and plasmids

The following antibodies were used: anti-β-tubulin (IF 1:100, WB 1:1000, LI-COR, cat# 926-42211), mice anti-CD63 antibody (IF 1:100, generous gift from Dr Andrew Peden, University of Sheffield, UK), anti-MKLP1 (IF 1:800, Santa Cruz Biotechnology, cat# sc-867) anti-FYCO1 (IF 1:100, WB 1:250, Bethyl Laboratories, cat# A302-796) and anti-LC3 (IF 1:200, WB 1:2000, NB100-2220). Phalloidin conjugated to Alexa Fluor 568 was from ThermoFisher Scientific (Waltham, MA, cat# A1238). FYCO1–GFP, FYCO1-FYVE deletion mutant and FYCO1-LIR deletion mutant DNA constructs were generous gifts from Terje Johansen, Institute of Medical Biology, University of Tromso, Norway. The Lamp1–mCherry DNA construct was received from Dr Andrew Peden.

Immunofluorescence and time-lapse microscopy

All fixed cells were imaged with an inverted Axiovert 200M microscope (Carl Zeiss) using a 63× oil immersion lens and QE charge-coupled device camera (Sensicam). *z*-stack images were taken at a step size of 100–500 nm. Image processing was performed by using the 3D rendering and exploration software Slidebook 5.0 (Intelligent Imaging Innovations).

For live-imaging, ∼50,000 GFP–FYCO1-, or GFP–FYCO1- and Lamp1–mCherry-expressing HeLa cells were plated on collagen-coated 6 cm glass-bottom dishes. For imaging, the dishes were placed in a heat- and humidity-controlled chamber (37°C, 5% CO_2 and 95% air). Cells were brought in focus using a 63× objective, and images were acquired either every 20 min or every 500 ms. In all cases, no more than 50 consecutive time-lapse images were obtained.

For immunofluorescence of whole-mount spheroids, spheroids were collected from the suspension culture and spotted onto poly-L-lysine-coated slide chambers to allow attachment. 3% paraformaldehyde (PFA) was used to fix spheroids prior to permeabilization with 0.5% Triton X-100 for 10 min at room temperature. Spheroids were washed three times with PBS/glycine rinse buffer (100 mM glycine in PBS) and blocked with PBS plus 10% FBS for 4 h at room temperature. Spheroids were stained with anti-MKLP-1 (cat# sc-867, Santa Cruz Biotechnology) at 1:800 concentration overnight at room temperature. The next day, spheroids were washed and stained with species-specific fluorescent-tag-conjugated secondary antibodies and mounted under coverslips. Analyses of MBs in spheroids were performed using Nikon TiE confocal microscopy. For optimal imaging of spheroids, a high NA water immersion 40× lens was used and pinhole size was set at 1.2 AU. *z*-stack images were taken at 0.5 µm step size and maximum intensity projection images were analyzed by using NIS-Elements Advanced Research software (Nikon) and Image J.

3D invadopodia formation assays

3D invadopodia formation assays were performed as previously described (Jacob et al., 2013, 2016). Briefly, 2.7×10^3 cells were seeded in Matrigel–collagen I mixture (3:1 ratio). The Matrigel–collagen–cell mixture was then spotted in eight-well chamber slides and allowed to harden for 45 min in a humidified 37°C incubator before adding DMEM supplemented with 10% FBS and 1% penicillin-streptomycin. Spheroids were allowed to grow for 4–5 days. Cells were then fixed and stained with Hoechst 33342, anti-tubulin antibodies and/or phalloidin conjugated to Alexa Fluor 568. The presence and number of invadopodia was quantified from randomly chosen spheroids. All data is derived from at least three different experiments.

Clonogenic assays

Approximately 100 cells were plated into each well of a six-well plate. Colonies were allowed to form for 7 days, then fixed with 10% neutral-buffered formalin. Colonies were stained with 0.1% Crystal Violet, washed and imaged. Colony formation quantitation was performed by using Metamorph (Molecular Devices, Sunnyvale, CA) software. The colony area was recorded and averaged from three different technical replicates in each experiment. The data shown are the means derived from three different experiments.

RNA isolation and quantitative PCR

RNA was isolated via TriZol extraction as per the manufacturers' instructions (Invitrogen, Carlsbad, CA). cDNA was obtained by using the iScript reverse transcriptase (Bio-Rad, Hercules, CA). Quantitative PCR (qPCR) was performed by using either TaqMan probes (Foster City, CA) or iTaq Universal SYBR Green (Bio-Rad, Hercules, CA) with primers obtained from PrimerDepot (Wenwu Cui, NIH). TaqMan probes used were: Mm00607939 (*Actb*) and Mm00530503 (*Fyco1*). Sequences used with SYBR green were: 5′-TCCTCTTTGCCTGAAACACC-3′ (human Fyco1-F), 5′-GGGCATGTCTTCAGTGTGCT (human Fyco1-R), 5′-CGCTCCGTGGCCTTAGC-3′ (human β-2 microglobin-F) and 5′-AATCTTTGGAGTACGCTGGATAGC-3′ (human β-2 microglobin-R). For quantification, Ct values were normalized to β-actin or β-2 microglobin then normalized to control cells.

Statistical analysis

All statistical analysis was performed in GraphPad Prism (GraphPad Software, San Diego, CA). A Student's *t*-test was used to determine significance for all datasets. In most cases, data shown are the mean±s.d. derived from at least three independent experiments. In assays analyzing individual cells, all cells were analyzed in three to five randomly chosen fields. Cells in these fields were either scored based on the phenotype or fluorescent intensity analysis, performed using Intelligent Imaging Innovations (Denver, CO) image analysis and rendering software.

Acknowledgements

We thank Dr Stephen Doxsey (University of Massachusetts) for sending us a HeLa cell line stably expressing MKLP1–GFP. We also thank Dr Johansen (University of Tromso, Norway) for FYCO1–GFP, FYCO1-LIR mutant and FYCO1-FYVE mutant cDNA. We are grateful to Dr Andrew Peden (University of Sheffield, UK) for mice anti-CD63 antibodies and the Lamp1–mCherry construct. We thank Dr Stephen Keysar for his assistance in culturing the CUHN013 cell line, and Dr Chao Liang as well as the University of Colorado Flow Cytometry Shared Resource for assistance with flow cytometry.

Competing interests

The authors declare no competing or financial interests.

Author contributions

Conceptualization: L.K.D., E.P., J.S., P.G., X.-J.W., R.P.; Methodology: L.K.D., E.P.; Validation: L.K.D., E.P.; Formal analysis: L.K.D., E.P., J.S., P.G., X.-J.W., R.P.; Investigation: L.K.D., E.P., J.S., P.G., A.J., X.-J.W., R.P.; Resources: A.J., X.-J.W., R.P.; Writing - original draft: L.K.D., E.P., X.-J.W., R.P.; Writing - review & editing: L.K.D., E.P., P.G., X.-J.W., R.P.; Supervision: V.A.S., A.J., X.-J.W., R.P.; Project administration: V.A.S., A.J., X.-J.W., R.P.; Funding acquisition: X.-J.W., R.P.

Funding

This work was supported in part by a grant from the National Institute of Diabetes and Digestive and Kidney Diseases (DK064380 to R.P.), Cancer League of Colorado foundation (Research Grant to R.P., X.-J.W.), the National Institutes of Health (DE15953 to X.-J.W. and DE24371 to X.-J.W. and A.J., R01CA149456 to A.J.), and Lietuvos Mokslo Taryba (APP7/2016 to V.A.S.). L.K.D. is supported by a National Cancer Institute T32 training grant (CA174648) and a research grant from Cancer League of Colorado Foundation. P.G. is supported by a WFS National Scholarship program. Deposited in PMC for release after 12 months.

Supplementary information

Supplementary information available online at
http://jcs.biologists.org/lookup/doi/10.1242/jcs.208983.supplemental

References

Akrap, N., Andersson, D., Bom, E., Gregersson, P., Ståhlberg, A. and Landberg, G. (2016). Identification of distinct breast cancer stem cell populations based on single-cell analyses of functionally enriched stem and progenitor pools. *Stem Cell Rep.* **6**, 121-136.

Bhutta, M., McInerny, C. and Gould, G. (2014). ESCRT function in cytokinesis: location, dynamics and regulation by mitotic kinases. *Int. J. Mol. Sci.* **15**, 21723-21739.

Biddle, A., Liang, X., Gammon, L., Fazil, B., Harper, L. J., Emich, H., Costea, D. E. and Mackenzie, I. C. (2011). Cancer stem cells in squamous cell carcinoma switch between two distinct phenotypes that are preferentially migratory or proliferative. *Cancer Res.* **71**, 5317-5326.

Blasky, A. J., Mangan, A. and Prekeris, R. (2015). Polarized protein transport and lumen formation during epithelial tissue morphogenesis. *Annu. Rev. Cell Dev. Biol.* **31**, 575-591.

Borowicz, S., Van Scoyk, M., Avasarala, S., Karuppusamy Rathinam, M. K., Tauler, J., Bikkavilli, R. K. and Winn, R. A. (2014). The soft agar colony formation assay. *J. Vis. Exp.* **92**, e51998.

Chen, C.-T., Ettinger, A. W., Huttner, W. B. and Doxsey, S. J. (2013). Resurrecting remnants: the lives of post-mitotic midbodies. *Trends Cell Biol.* **23**, 118-128.

Chen, J., Ma, Z., Jiao, X., Fariss, R., Kantorow, W. L., Kantorow, M., Pras, E., Frydman, M., Pras, E., Riazuddin, S. et al. (2011). Mutations in FYCO1 cause autosomal-recessive congenital cataracts. *Am. J. Hum. Genet.* **88**, 827-838.

Crowell, E. F., Gaffuri, A.-L., Gayraud-morel, B., Tajbakhsh, S. and Echard, A. (2014). Engulfment of the midbody remnant after cytokinesis in mammalian cells. *J. Cell Sci.* **127**, 3840-3851.

Da Ros, M., Lehtiniemi, T., Olotu, O., Fischer, D., Zhang, F.-P., Vihinen, H., Jokitalo, E., Sironen A., Toppari J. and Kotaja N. (2017). FYCO1 and autophagy control the integrity of the haploid male germ cell-specific RNP granules. *Autophagy* **13**, 302-321.

D'Avino, P. P. and Capalbo, L. (2016). Regulation of midbody formation and function by mitotic kinases. *Semin. Cell Dev. Biol.* **53**, 57-63.

Dionne, L. K., Wang, X.-J. and Prekeris, R. (2015). Midbody: from cellular junk to regulator of cell polarity and cell fate. *Curr. Opin. Cell Biol.* **35**, 51-58.

Douglas, M. E. and Mishima, M. (2010). Still entangled: assembly of the central spindle by multiple microtubule modulators. *Semin. Cell Dev. Biol.* **21**, 899-908.

Ettinger, A. W., Wilsch-Bräuninger, M., Marzesco, A.-M., Bickle, M., Lohmann, A., Maliga, Z., Karbanová, J., Corbeil, D., Hyman, A. A. and Huttner, W. B. (2011). Proliferating versus differentiating stem and cancer cells exhibit distinct midbody-release behaviour. *Nat. Commun.* **2**, 503.

Fazeli, G., Trinkwalder, M., Irmisch, L. and Wehman, A. M. (2016). C. elegans midbodies are released, phagocytosed and undergo LC3-dependent degradation independent of macroautophagy. *J. Cell Sci.* **129**, 3721-3731.

Fededa, J. P. and Gerlich, D. W. (2012). Molecular control of animal cell cytokinesis. *Nat. Cell Biol.* **14**, 440-447.

Franken, N. A. P., Rodermond, H. M., Stap, J., Haveman, J. and van Bree, C. (2006). Clonogenic assay of cells in vitro. *Nat. Protoc.* **1**, 2315-2319.

Güttsches, A.-K., Brady, S., Krause, K., Maerkens, A., Uszkoreit, J., Eisenacher, M., Schreiner, A., Galozzi, S., Mertens-Rill, J., Tegenthoff, M. et al. (2016). Proteomics of rimmed vacuoles define new risk allele in inclusion body myositis. *Ann. Neurol.* **81**, 227-239.

Hu, C.-K., Coughlin, M. and Mitchison, T. J. (2012). Midbody assembly and its regulation during cytokinesis. *Mol. Biol. Cell* **23**, 1024-1034.

Jacob, A., Jing, J., Lee, J., Schedin, P., Gilbert, S. M., Peden, A. A., Junutula, J. R. and Prekeris, R. (2013). Rab40b regulates trafficking of MMP2 and MMP9 during invadopodia formation and invasion of breast cancer cells. *J. Cell Sci.* **126**, 4647-4658.

Jacob, A., Linklater, E., Bayless, B. A., Lyons, T. and Prekeris, R. (2016). The role and regulation of Rab40b/Tks5 complex during invadopodia formation and cancer cell invasion. *J. Cell Sci.* **129**, 4341-4353.

Kuo, T.-C., Chen, C.-T., Baron, D., Onder, T. T., Loewer, S., Almeida, S., Weismann, C. M., Xu, P., Houghton, J.-M., Gao, F.-B. et al. (2011). Midbody accumulation through evasion of autophagy contributes to cellular reprogramming and tumorigenicity. *Nat. Cell Biol.* **13**, 1214-1223.

Li, D., Mangan, A., Cicchini, L., Margolis, B. and Prekeris, R. (2014). FIP5 phosphorylation during mitosis regulates apical trafficking and lumenogenesis. *EMBO Rep.* **15**, 428-437.

Ma, J., Becker, C., Reyes, C. and Underhill, D. M. (2017). Cutting edge: FYCO1 recruitment to Dectin-1 Phagosomes is accelerated by light chain 3 protein and regulates phagosome maturation and reactive oxygen production. *J. Immunol.* **192**, 1356-1360.

Mangan, A. J., Sietsema, D. V., Li, D., Moore, J. K., Citi, S. and Prekeris, R. (2016). Cingulin and actin mediate midbody-dependent apical lumen formation during polarization of epithelial cells. *Nat. Commun.* **7**, 12426.

Mierzwa, B. and Gerlich, D. W. (2014). Cytokinetic abscission: molecular mechanisms and temporal control. *Dev. Cell* **31**, 525-538.

Olsvik, H. L., Lamark, T., Takagi, K., Larsen, K. B., Evjen, G., Øvervatn A., Mizushima T. and Johansen T. (2015). FYCO1 contains a C-terminally extended, LC3A/B-preferring LC3-Interacting Region (LIR) motif required for efficient maturation of autophagosomes during basal autophagy. *J. Biol. Chem.* **290**, 29361-29374.

Pankiv, S., Alemu, E. A., Brech, A., Bruun, J.-A., Lamark, T., Øvervatn, A., Bjørkøy, G. and Johansen, T. (2010). FYCO1 is a Rab7 effector that binds to LC3 and PI3P to mediate microtubule plus end–directed vesicle transport. *J. Cell Biol.* **188**, 253-269.

Pohl, C. and Jentsch, S. (2009). Midbody ring disposal by autophagy is a post-abscission event of cytokinesis. *Nat. Cell Biol.* **11**, 65-70.

Pollarolo, G., Schulz, J. G., Munck, S. and Dotti, C. G. (2011). Cytokinesis remnants define first neuronal asymmetry in vivo. *Nat. Neurosci.* **14**, 1525-1533.

Salzmann, V., Chen, C., Chiang, C.-Y. A., Tiyaboonchai, A., Mayer, M. and Yamashita, Y. M. (2014). Centrosome-dependent asymmetric inheritance of the midbody ring in Drosophila germline stem cell division. *Mol. Biol. Cell* **25**, 267-275.

Schiel, J. A., Park, K., Morphew, M. K., Reid, E., Hoenger, A. and Prekeris, R. (2011). Endocytic membrane fusion and buckling-induced microtubule severing mediate cell abscission. *J. Cell Sci.* **124**, 1411-1424.

Schiel, J. A., Simon, G. C., Zaharris, C., Weisz, J., Castle, D., Wu, C. C. and Prekeris, R. (2012). FIP3-endosome-dependent formation of the secondary ingression mediates ESCRT-III recruitment during cytokinesis. *Nat. Cell Biol.* **14**, 1068-1078.

White, R. A., Neiman, J. M., Reddi, A., Han, G., Birlea, S., Mitra, D., Dionne, L. K., Fernandez, P., Murao, K., Bian, L. et al. (2013). Epithelial stem cell mutations that promote squamous cell carcinoma metastasis. *J. Clin. Invest.* **123**, 4390-4404.

Supplemental Figure 1

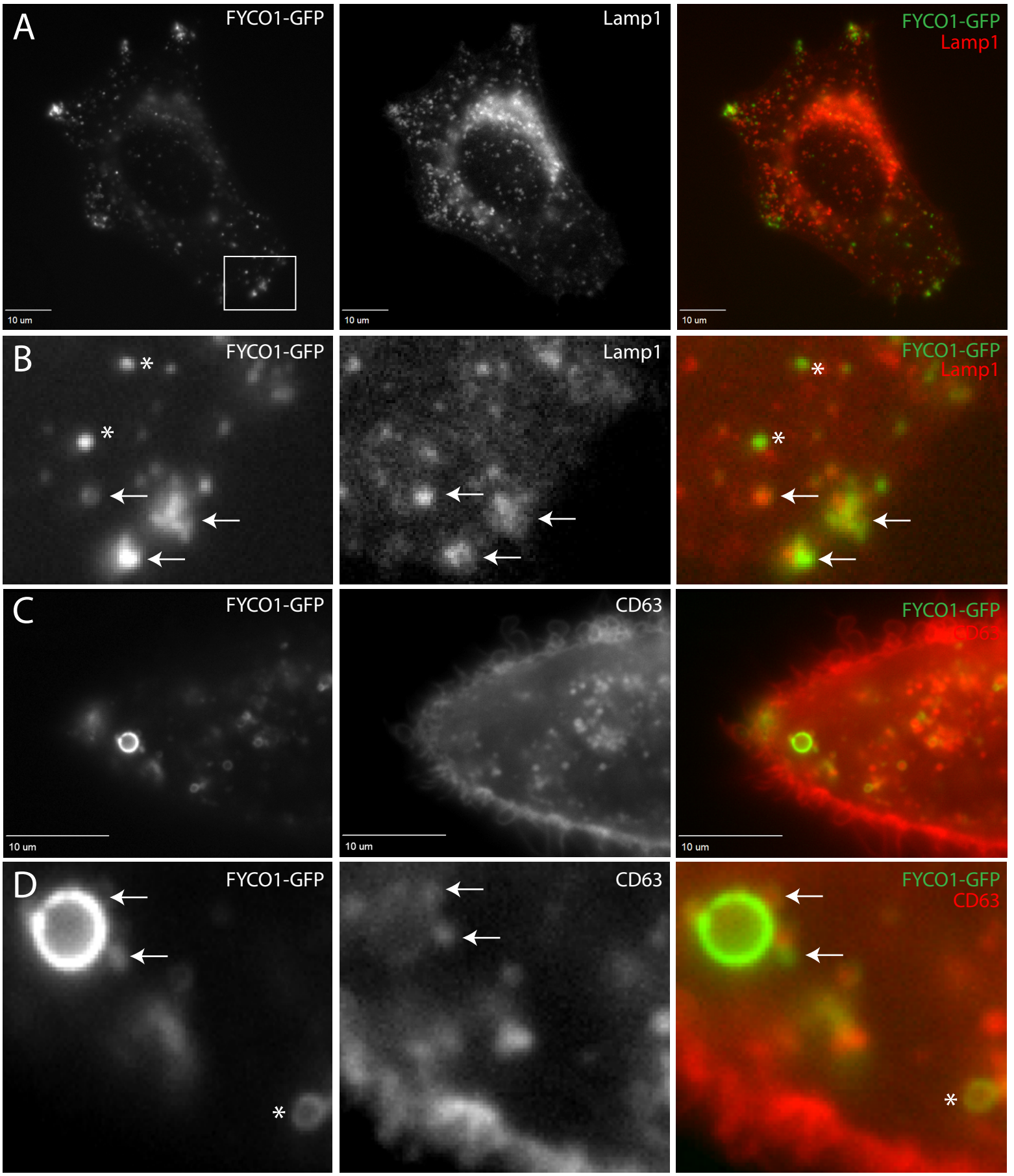

Supplementary Figure 1. Partial FYCO1 co-localization with Lamp1.
HeLa cells were transiently co-transfected with FYCO1-GFP and then fixed and stained with two different lysosomal markers, ant-Lamp1 (A and B) and anti-CD63 (C and D) antibodies. The presence of lysosomal marker in FYCO1-associated organelles was the analyzed. Panels B and D show higher magnification image of the area boxed in panel A and C. Arrows point to organelles containing both FYCO1-GFP and Lamp1 or FYCO1-GFP and CD63. Asterisks mark organelle containing only FYCO1-GFP but not Lamp1 or CD63.

Journal of Cell Science • Supplementary information

Supplemental Figure 2

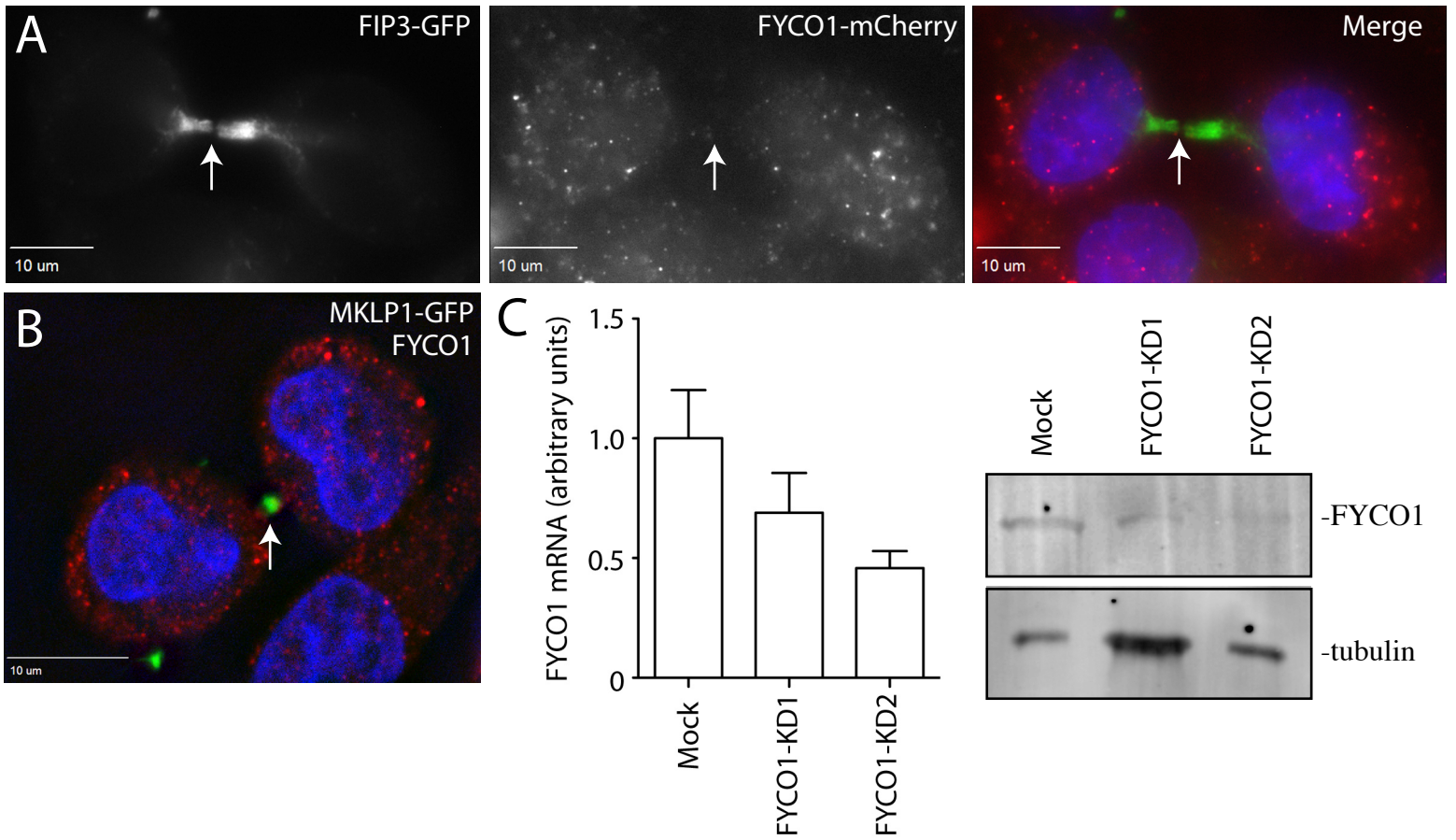

Supplementary Figure 2. FYCO1 knock-down does not affect cytokinesis or autophagic flux.

(A) To test whether FYCO1 is present at the midbody during cytokinesis HeLa cells expressing FIP3-GFP (furrow endosome marker) and FYCO1-mCherry were fixed and analyzed for FYCO1 localization. Arrows mark the MB.

(B) To test whether FYCO1 is present at the midbody during cytokinesis HeLa cells expressing MKLP1-GFP (MB marker) were fixed and stained with anti-FYCO1 antibody. Arrow marks the MB.

(C) Quantitative PCR and western blots assessing FYCO1 mRNA levels in HeLa cells stably expressing two different FYCO1 shRNAs. Data shown are the means and standard deviations.

(D) To test whether FYCO1 knock-down affects cytokinesis control cells or FYCO1 shRNA-expressing cells were stained with anti-acetylated tubulin and Hoechst 33342. Number of multi-nucleated cells or cells in the telophase were then counted. Data shown are the means and standard deviations from three independent experiments.

(E) To test effect of FYCO1 knock-down on autophagic flux cells were grown in the presence or absence of 40 μM chloroquine for 4 hours. Cells were then lysed and levels of LC3-II (activated LC3) was analyzed by western blotting.

Journal of Cell Science • Supplementary information

Supplemental Figure 3

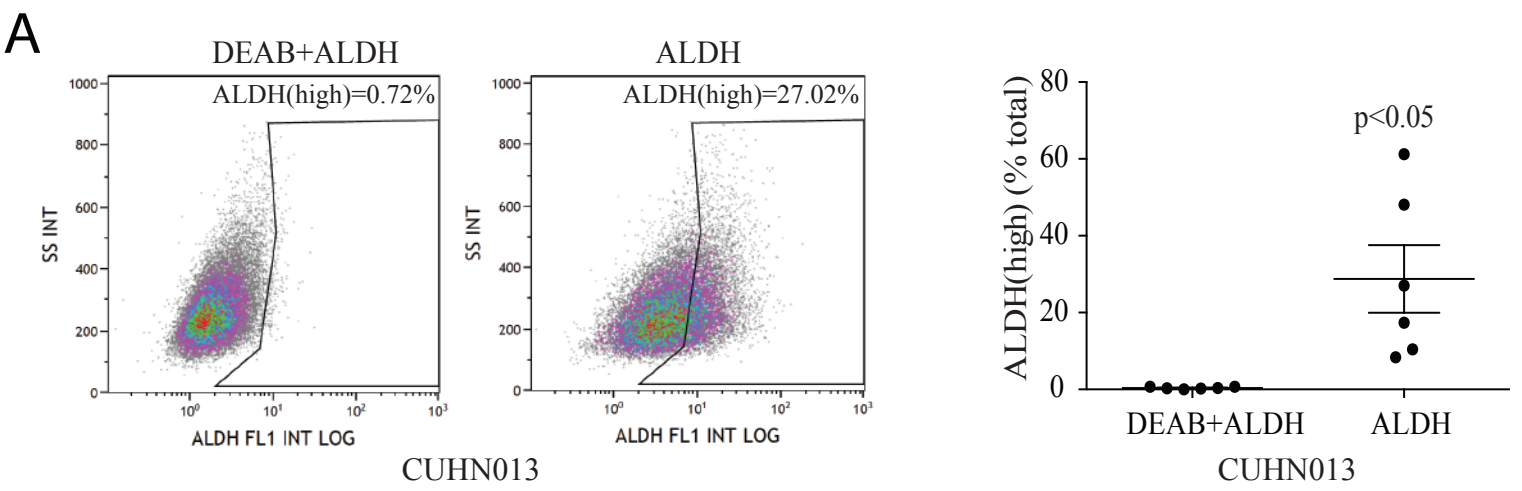

Supplementary Figure 3. ALDH(high) population of CUHN013 squamous cell carcinoma accumulate post-mitotic MBs

(A) Flow cytometry analysis of ALDH(high) cells in CUHN013. Cells were incubated in the dark with ALDEFLUOR assay buffer containing the activated ALDEFLUOR substrate, with or without ALDH inhibitor diethylaminobenzaldehyde (DEAB). Cells were flow sorted to identify ALDH(high) and ALDH(low) populations. Data shown are the means and standard deviations from six independent experiments.

(B) Flow sorted ALDH(high) and ALDH(low) CUHN013 cells were cultured on Ultra Low Attachment six-well plates to allow formation of spheroids (top panels). Note that ALDH(high) form larger spheroids than ALDH(low). The spheroids were then fixed and stained with anti-MKLP1 antibodies to visualize post-mitotic MBs. Images shown are maximum intensity projection along the z-axis. Bar graph shows quantification of MB number in CUHN013 ALDH(high) and ALDH(low)-derived spheroids. Data shown are the average number of MBs per spheroid area. Data shown are the means and standard deviations from three independent experiments.

Journal of Cell Science • Supplementary information

Supplemental Figure 4

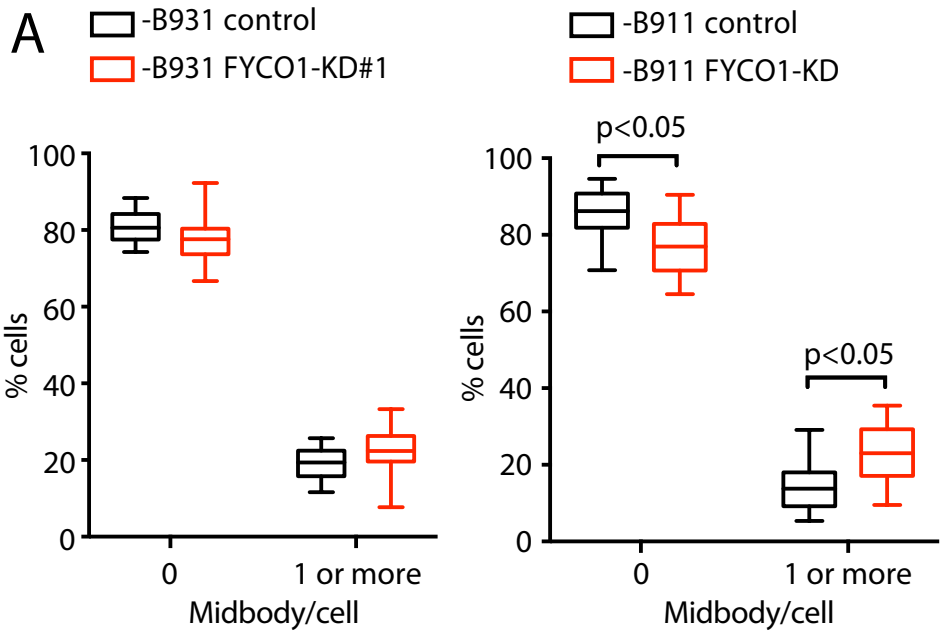

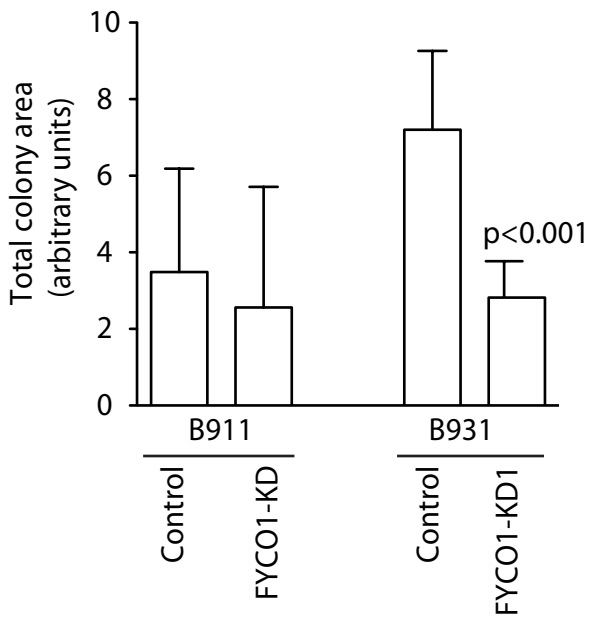

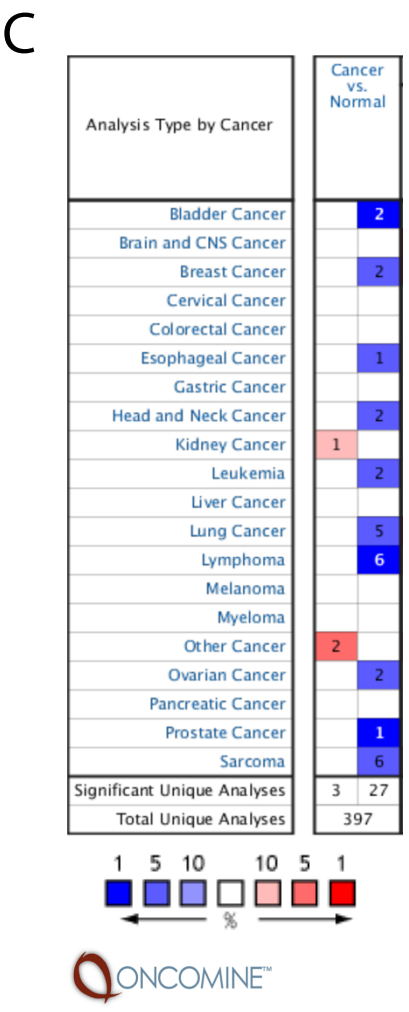

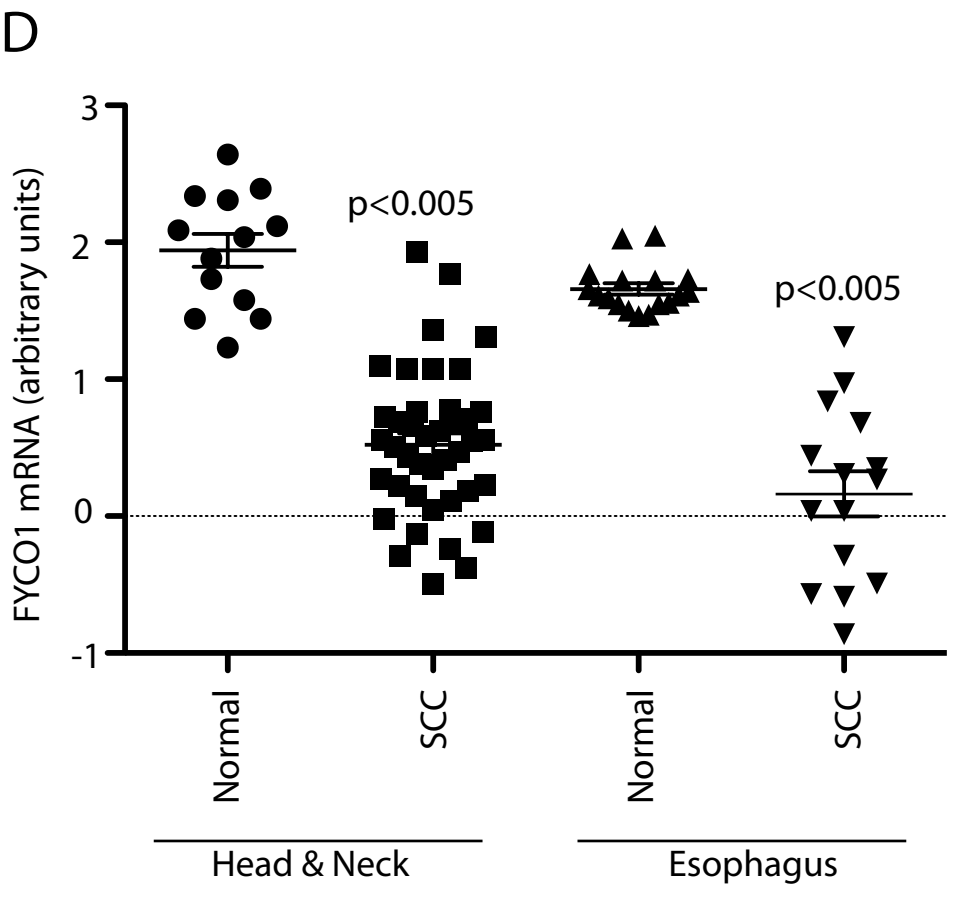

Supplemental Figure 4. FYCO1 is down-regulated in many cancers including squamous cell carcinomas.
(A) B911 and B931 cells stably expressing FYCO1 shRNAs cells were analyzed for the absence or presence of post-mitotic MBs as determined by staining with anti-MKLP1 antibody. The vertical segments in box plots show the first quartile, median, and third quartile. The whiskers on both ends represent the maximum and minimum values for each dataset analyzed from three independent experiments.
(B) To test the effect of FYCO1 knock-down on stemness of B911 and B931 cells, mock or FYCO1 shRNA-expressing cells were plated in 6 well plates at the dilution of 100 cells per well. Cells were allowed grow for one week and then stained with 0.1% crystal violet. The number and size of colonies and then quantified by Metamorph. Data shown are the means and standard deviations from three independent experiments.
(C) Messenger RNA levels of FYCO1 in various cancers as compared to normal tissue. The data shown was obtained using data mining by Oncomine.
(D) Messenger RNA levels of FYCO1 in head & neck and esophagus squamous cell carcinomas as compared to normal tissue. The data shown was obtained using data mining by Oncomine.